DOI 10.1007/s10946-020-09875-9
Journal of Russian Laser Research, Volume 41, Number 3, May, 2020

ALL-SOLID-STATE *Q*-SWITCHED LASER OPERATING AT 294.6 nm

Ji Yao,[1,2] Quan Zheng,[1,3*] Qi Li,[3] Yu-ning Wang,[3] Xi Chen,[3] Yi Yao,[3] and Wei Huang[1]

[1] *Changchun Institute of Optics, Fine Mechanics and Physics, Chinese Academy of Sciences Changchun 130033, Jilin, China*

[2] *University of Chinese Academy of Sciences Beijing 100190, China*

[3] *Changchun New Industries Optoelectronics Tech. Co., Ltd. Changchun 130012, China*

*Corresponding author e-mail: zhengquan@cnilaser.com

Abstract

We report a stable high-power all-solid-state *Q*-switched laser operating at 294.6 nm with a pulse width of 24 ns and a repetition rate of 20 kHz produced by intracavity sum-frequency generation and external frequency doubling in LiB_3O_5 and β-BaB_2O_4 crystals, respectively. Upon synchronizing the fundamental lasers, the maximum output power at 589 nm is 1.2 W, which is frequency doubled to produce up to 167.8 mW at 294.6 nm, thereby providing a conversion efficiency of 13.98%.

Keywords: ultraviolet lasers, high power, frequency doubling.

1. Introduction

Now ultraviolet (UV) lasers are extensively discussed due to their wide range of applications in spectroscopy, environmental sensing, and chemical detection [1–3]. In particular, tunable continuous-wave (CW) lasers at 295 nm are used for cooling and collimating gallium atoms, as well as for lidars [4–6]. Nowadays, there are two ways to produce a tunable CW 295-nm laser generation, namely, (i) frequency doubling of a rhodamine 6G dye laser with a fundamental wavelength of 589 nm and (ii) fourth-harmonic generation of an optically-pumped semiconductor laser with a fundamental wavelength of 1178 nm [7, 8]. Compared with CW UV lasers at 295 nm, nanosecond pulsed lasers offer higher peak power and higher detection sensitivity but unfortunately only few reports to date have discussed such lasers. To fill this void, we discuss herein a 167.8 mW all-solid-state nanosecond 294.6-nm pulsed laser, which is achieved by external-cavity frequency doubling in a β-BaB_2O_4 (BBO) crystal of a 589 nm fundamental laser, itself generated by intracavity sum-frequency generation (SFG) of 1064 and 1319 nm lasers [9, 10].

2. Experimental Setup

Figure 1 shows an overall schematic of the 294.6 nm laser system, which comprises (i) an SFG subsystem and (ii) a frequency-doubling subsystem.

2.1. Sum-Frequency Subsystem

Manuscript submitted by the authors in English first on February 23, 2020 and in final form on March 23, 2020.

The SFG subsystem comprises (i) a 1064 nm Q-switched laser, (ii) a 1319 nm Q-switched laser, and (iii) a 589 nm intracavity SFG system. The 1319 nm laser consists of a pump source comprising a semiconductor laser at 808 nm and a combination of coupling lenses, a Nd:YAG (∅3×3×5 mm) gain medium doped with 1% Nd^{3+}, and the pumping side is antireflection (AR) coated at 808 nm and high-reflection (HR) coated at 1319 nm; the other side is AR coated at 808 and 1319 nm. A 1319 nm acousto-optic Q-switch is used to generate the nanosecond pulses. In addition, there are a coupling mirror with a HR coating at 1319 nm and an AR coating at 1064 nm (M1), a plane HR mirror that is HR coated at 1319, 1064, and 589 nm (M2), and an output coupling mirror that is HR coated at both 1319 and 1064 nm and AR coated at 589 nm (M3).

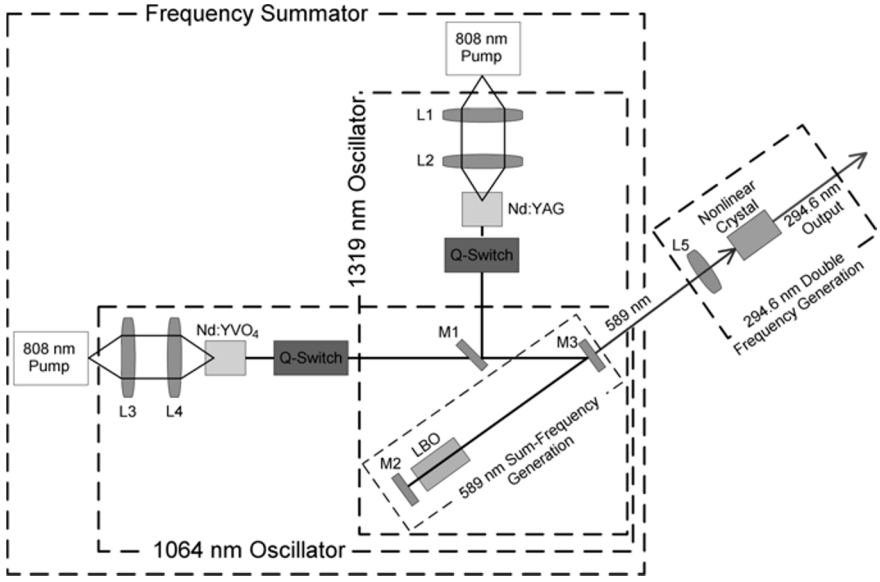

Fig. 1. Schematic of 294.5 nm laser system. Here, M1 is a mirror 45° HR coated at 1319 nm and an AR coated at 1064 nm, M2 is a mirror HR coated at 1319, 1064, and 589 nm, and M3 is a mirror HR coated at both 1319 and 1064 nm and AR coated at 589 nm.

The construction and features of the 1064 nm laser are similar to those of the 1319 nm laser, except the coating and gain medium. This laser produces linearly polarized 1064 nm optical pulses when Nd:YVO_4 is used as the gain medium, and it is used to improve the SFG conversion efficiency.

The 589 nm intracavity SFG subsystem includes the overlapping 1064 and 1319 nm oscillators and an LiB_3O_5 (LBO) crystal (2×2×10 mm, $\theta = 90°$, $\varphi = 0°$) that, given its low absorption, high damage threshold, and high nonlinear coefficient, is used as the nonlinear crystal for SFG [11].

To improve the output power at 589 nm, the LBO crystal is placed close to mirror M2, at the primary waist of the fundamental laser. The cavity length is designed and optimized employing the ABCD matrix theory. Figure 2 shows the fundamental beam widths in both the gain medium and LBO, where we see that the fundamental-beam waists differ only slightly in the LBO. Note also that the spot size remains relatively constant as a function of the thermal-lens focal length, and the beam widths of the fundamental beams in the gain medium are well matched with that of the pump.

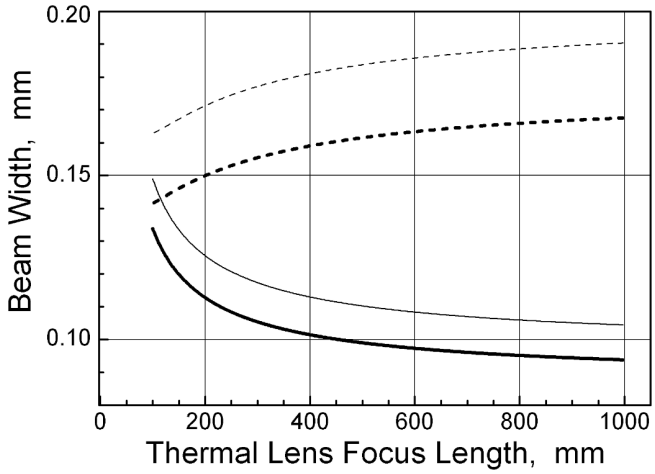

Fig. 2. Width of the fundamental beam waist in the gain medium (dashed curves) and LBO crystal (solid curves) for 1319 nm beam (thin curves) and 1064 nm beam (bold curves).

Finally, pulse synchronization technology is used in the SFG setup to synchronize the two fundamental lasers.

3. Frequency-Doubling Subsystem

The frequency-doubling system comprises a converging lens and a nonlinear crystal. BBO, CsB_3O_5 (CBO), $CsLiB_6O_{10}$ (CLBO), $KBe_2BO_3F_2$, and LBO were considered as nonlinear crystals for frequency doubling to 589 nm. Table 1 lists the phase-matching mode, effective nonlinear coefficient d_{eff}, walk-off angle, and acceptance angle. BBO offers the largest d_{eff} and walk-off angle, as well as the smallest acceptance angle. CBO offers a larger d_{eff} and acceptance angle, and the smallest walk-off angle (0°). The other crystals are eliminated because of their low d_{eff}. Although it has larger walk-off and acceptance angle, BBO is chosen for frequency doubling in this experiment because of its large effective nonlinear coefficient and associated mature-growth technology and commercial applications. Lens 5 focuses the 589 nm beam into the BBO crystal to enhance the incident power density. A 294.6 nm laser beam is produced upon injecting the SFG 589 nm laser beam into the BBO crystal (2×2×10 mm, $\theta = 41.5°$), which is AR coated at 589 nm.

Table 1. Parameters of Nonlinear Crystals.

	Phase-matching mode	d_{eff} [pm/V]	Walk-off angle [mrad]	Acceptance angle [mrad·cm]
BBO	o + o → e	1.87	83.01	0.42
CBO	e + e → o	−1.14	0	1.88
CLBO	o + o → e	0.685	37.55	1.05
LBO	o + o → e	0.376	14.57	2.5

4. Experimental Results

We measured the 1064 and 1319 nm pulse profiles using a photodetector connected to a digital oscilloscope, as shown in Fig. 3. Figure 3 a shows the appearance of a 1064 nm pulse 1.051 μs before the pulse at 1319 nm, which results from a high inversion-population density and a low threshold at 1064 nm. A pulse synchronizer was used to synchronize the fundamental lasers. The pulse synchronizer emits two square signals to control the repetition frequency and triggering time of the Q-switches, then it controls the time difference between the 1064 and 1319 nm laser generation by adjusting the delay time of the signals, with the result shown in Fig. 3 b after delaying the 1064 nm pulse by 1.06 μs. With this pulse delay, the maximum output power at 589 nm is 1.2 W.

Figure 4 shows the experimental results for the conversion efficiency with different values of the input power I. As shown in Fig. 4 a and b, a maximum output power 167.8 mW at 294.6 nm is obtained with an input power of 1.2 W, thereby giving a conversion efficiency of 13.98%. Figure 4 c and d shows the central wavelength and pulse profile of the final output.

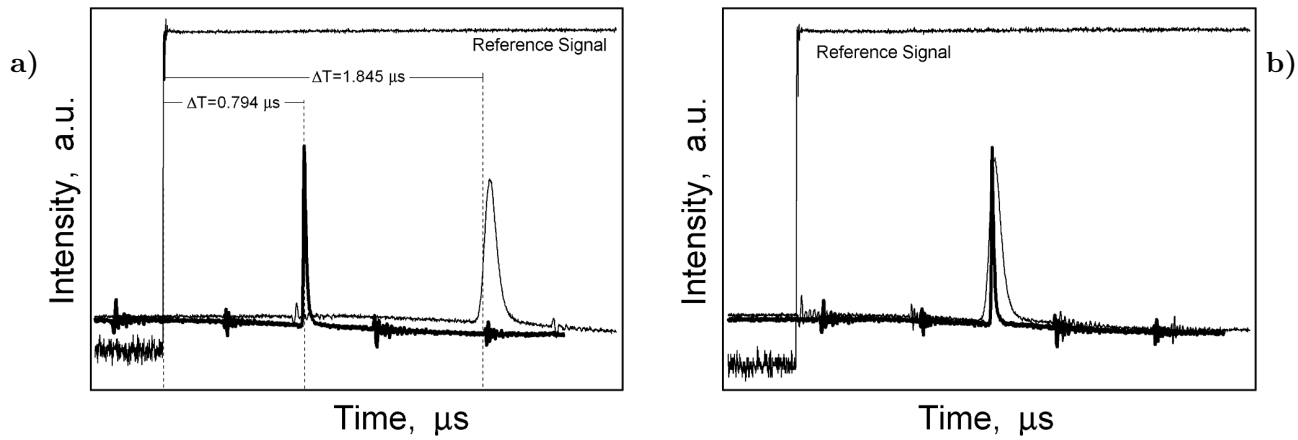

Fig. 3. Pulse profiles for 1064 and 1319 nm without delay (a) and with a delay of 1.06 μs (b). 1064 nm pulse profile is shown by the grey curve and 1319 nm – by the thin curve.

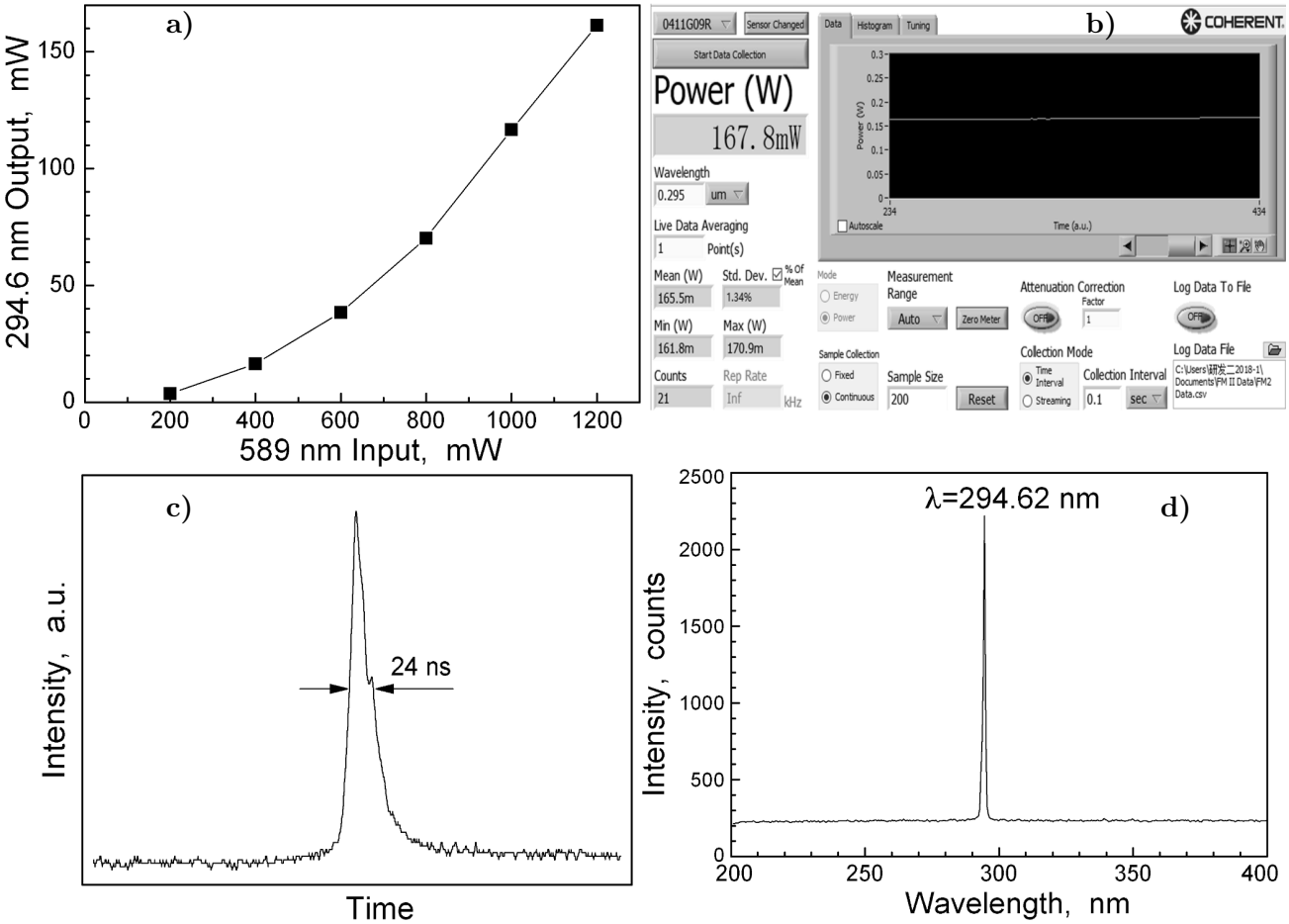

Fig. 4. Output power versus the input power for frequency doubling in BBO crystal (a), the maximum output power (b), the profile of 294.6 nm pulse (c), and the spectrum of 294.6 nm pulse (d).

5. Conclusions

In summary, we demonstrated an all-solid-state Q-switched laser operating at 294.6 nm produced by intracavity SFG and external frequency doubling, using LBO and BBO crystals, respectively. The maximum output power is 167.8 mW at 294.6 nm with a repetition rate of 20 kHz and a pulse width of 24 ns.

References

1. H. Wako, S. I. Ishiuchi, D. Kato, et al., *Phys. Chem. Chem. Phys.*, **19**, 10777 (2017).
2. H. Liu, W. Yuan, F. Cheng, et al., *J. Phys. B: At. Mol. Opt. Phys.*, **51**, 225002 (2018).
3. A. Steube, T. Schenk, A. Tretyakov, and H. P. Saluz, *Nat. Commun.*, **8**, 1303 (2017).
4. S. J. Rehse, *Light Force Manipulation of Gallium Atoms*, PhD Thesis, Colorado State University (2002).
5. S. J. Rehse, K. M. Bockel, and S. A. Lee, *Phys. Rev. A*, **69**, 666 (2004).
6. R. De Young, W. Carrion, D. Pliutau, and R. Ganoe, "Solid state mobile lidar for ozone atmospheric profiling," Talk at CLEO Applications and Technology Conference, 8–13 June 2014, San Jose, California, USA, p. AF1P-2.
7. S. J. Rehse and S. A. Lee, *Opt. Commun.*, **213**, 347 (2002).
8. Y. Kaneda, M. Fallahi, J. Hader, et al., *Opt. Lett.*, **34**, 3511 (2009).
9. Y. Wang, Q. Zheng, Y. Yao, and X. Chen, *Appl. Opt.*, **52**, 1876 (2013).
10. X. Chen, X. Li, H. Zhang, et al., *Chin. Opt. Lett.*, **7**, 815 (2009).
11. W. Peng-Yuan, X. Shi-Yong, B. Yong, et al., *Chin. Phys. B*, **23**, 094208 (2014).
12. W. Koechner, *Solid-State Laser Engineering*, 6th ed., Springer (2006).
13. G. S. Zhong and X. Mao, *Laser Technol.*, **37**, 766 (2013).
14. J. A. Armstrong, N. Bloembergen, J. Ducuing, and P. S. Pershan, *Phys. Rev.*, **127**, 1918 (1962).